



# HHS Public Access

Author manuscript

*J Mass Spectrom.* Author manuscript; available in PMC 2017 September 05.

Published in final edited form as:

*J Mass Spectrom.* 2016 August ; 51(8): 535–548. doi:10.1002/jms.3780.

## Training in metabolomics research. II. Processing and statistical analysis of metabolomics data, metabolite identification, pathway analysis, applications of metabolomics and its future

Stephen Barnes<sup>1,4,6,\*</sup>, H. Paul Benton<sup>10</sup>, Krista Casazza<sup>3</sup>, Sara Cooper<sup>7</sup>, Xiangqin Cui<sup>5</sup>, Xiuxia Du<sup>8</sup>, Jeffrey Engler<sup>1</sup>, Janusz H. Kabarowski<sup>2</sup>, Shuzhao Li<sup>9</sup>, Wimal Pathmasiri<sup>11</sup>, Jeevan K. Prasain<sup>4,6</sup>, Matthew B. Renfrow<sup>1</sup>, and Hemant K. Tiwari<sup>5</sup>

<sup>1</sup>Department of Biochemistry and Molecular Genetics, University of Alabama at Birmingham, Birmingham, AL 35294

<sup>2</sup>Department of Microbiology, University of Alabama at Birmingham, Birmingham, AL 35294

<sup>3</sup>Department of Pediatrics, University of Alabama at Birmingham, Birmingham, AL 35294

<sup>4</sup>Department of Pharmacology and Toxicology, University of Alabama at Birmingham, Birmingham, AL 35294

<sup>5</sup>School of Medicine; Section on Statistical Genetics, School of Public Health, University of Alabama at Birmingham, Birmingham, AL 35294

<sup>6</sup>Targeted Metabolomics and Proteomics Laboratory, University of Alabama at Birmingham, Birmingham, AL 35294

<sup>7</sup>HudsonAlpha, Huntsville, AL 35806

<sup>8</sup>Department of Bioinformatics and Genomics, University of North Carolina at Charlotte, NC 28223

<sup>9</sup>Department of Medicine, Emory University, Atlanta, GA 30322

<sup>10</sup>Scripps Research Institute, La Jolla, CA 92307

<sup>11</sup>RTI International, Research Triangle Park, NC 27709

### Abstract

Metabolomics, a systems biology discipline representing analysis of known and unknown pathways of metabolism, has grown tremendously over the past 20 years. Because of its comprehensive nature, metabolomics requires careful consideration of the question(s) being asked, the scale needed to answer the question(s), collection and storage of the sample specimens, methods for extraction of the metabolites from biological matrices, the analytical method(s) to be employed and the quality control of the analyses, how collected data are correlated, the statistical methods to determine metabolites undergoing significant change, putative identification of metabolites, and the use of stable isotopes to aid in verifying metabolite identity and establishing

\*Author for Correspondence: Stephen Barnes, PhD, Department of Pharmacology and Toxicology, MCLM 452, University of Alabama at Birmingham, 1918 University Boulevard, Birmingham, AL 35294, Tel #: 205 934-7117; Fax #: 205 934-6944; sbarnes@uab.edu.

pathway connections and fluxes. This second part of a comprehensive description of the methods of metabolomics focuses on data analysis, emerging methods in metabolomics and the future of this discipline.

## Introduction

This is the second part of a summary of a training workshop on metabolomics published in the previous issue of the *Journal of Mass Spectrometry*<sup>1</sup>. The workshop, supported by a R25 grant from the NIH Common Fund Program in Metabolomics, has been held each summer at the University of Alabama in Birmingham since 2013. It is focused on the analysis of metabolomics data collected using NMR and MS platforms as well as other applications of metabolomics, the future of metabolomics, and other training opportunities for interested investigators.

## 1. Data Analysis

### a. <sup>1</sup>H-NMR

Derivation of metabolomics data from NMR spectra is the use of chemometric analysis<sup>2, 3</sup>. After spectral pre-processing during which the added internal standard, e.g., DSS, is assigned to 0 ppm, the NMR spectra are “binned” using a defined interval (e.g., 0.4 ppm) (Fig. 1). This can be achieved using a number of different commercially software platforms including ACD<sup>[1]</sup> ([www.acdlabs.com](http://www.acdlabs.com)), Chenomx ([www.chenomx.com](http://www.chenomx.com)) and MestreNova (<http://mestrelab.com/>). NMR spectra also contain several elements which may need to be removed prior to statistical analysis. These come from the protons in water, urea (in the case of urine), protons resonances of noise regions upfield to the DSS peak and those that are downfield from most metabolites (Fig. 1). Another issue can be the pH of the sample, particularly in urine. NMR peak alignment tools<sup>4, 5</sup> are helpful to overcome issues with pH based chemical shift variation. By adding imidazole, the chemical shift of its protons allows the adjustment of other proton resonances susceptible to pH enabling identification using pH sensitive NMR libraries such as Chenomx. Another way is to use a buffer solution to control pH.

Untargeted NMR metabolomics analysis is typically performed in a high throughput manner by binning NMR data. Resulting “bin” data can be used as the input for principal component analysis (PCA) and partial least squares discriminant analysis (PLS-DA) or orthogonal partial least squares discriminant analysis (OPLS-DA) to determine the extent of differences between experimental groups and to identify the metabolic features that are important for distinguishing the study groups. The NMR data are mean centered and scaled (unit variance or Pareto) prior to multivariate data analysis.

A particular advantage of NMR metabolomics is that it is quantitative. The summed area of the peaks associated with each metabolite is representative of its concentration when referenced to an internal standard like DSS. Chenomx software can be used to pre-process

---

<sup>1</sup>ACD has a free academic version

and profile NMR spectra to identify and quantify metabolites. Metabolite concentrations can then be used for parametric statistics.

## b. LC-MS and GC-MS

The goal of data pre-processing is to extract information about metabolite ions from raw mass spectrometry data. The raw data consists of a series of mass spectra each of which is acquired at a specific time and thus has a scan acquisition time (i.e., retention time) associated with it. Together with the mass-to-charge ratio and relative abundance of each mass-to-charge ratio, the raw data are three-dimensional.

Data pre-processing mostly occurs in two-dimensional spaces. The first two-dimensional space is the mass-to-charge ratio and relative abundance for each particular retention time, i.e., processing occurs at the spectrum level. The second is the retention time and relative abundance for a particular mass-to-charge ratio or all of the mass-to-charge ratios. The relationship between the retention time and the summation of relative abundance values for all of the mass-to-charge ratios gives rise to the total ion chromatogram (TIC). The relationship between the retention time and relative abundance values for a particular mass-to-charge ratio gives rise to the extracted ion chromatogram (EIC).

The data processing workflow consists of a sequence of steps as depicted in Figure 2. Centroiding concerns converting spectral data in profile mode to centroid mode by determining the most likely mass values detected in each spectrum. The subsequent steps about features start from detecting all of the chromatographic peak features in each EIC.

For mass analyzers with unit mass measurement accuracy, an EIC can be easily obtained by extracting each unit mass and its relative abundance value over time. For mass analyzers with high mass measurement accuracy, there are two approaches. The first approach is through mass binning. Basically, the mass axis is divided into equal bins and all of the mass-to-charge ratios that fall into one mass bin and their corresponding relative abundance values give rise to an EIC. The advantage of this approach is that the algorithm is easy to implement and all of the EICs in a dataset can be rapidly built. The disadvantage is that both EIC splitting and merging can happen. Splitting occurs when a binning boundary separates mass-to-charge ratios that belong to the same mass into two different bins. Merging occurs when mass-to-charge ratios that belong to two different masses are sandwiched between two adjacent binning boundaries. There are methods to avoid these issues by combining adjacent bins ( $n, n+1$ ) to check for peaks. This method, *matchedFilter*, was used in the widely used software tool, XCMS<sup>6</sup>.

A second, more sophisticated approach to building EICs is to automatically determine the binning boundaries. Toward this end, XCMS now uses an intelligent binning algorithm (*centWave*) to find areas of interest<sup>7</sup>. These areas are found by a tracking algorithm that looks for a smooth slope with a small amount of  $m/z$  drift. Once this pass is made over the single LC/MS spectrum, a second algorithm is used to integrate the peak. A series of wavelets are fitted to the peak until the best wavelet is found. If no wavelet was fitted successfully, then the area is not a peak. Some areas contain co-eluting peaks and the wavelets are able to pull these peaks apart. This approach overcomes the disadvantages of

the aforementioned binning at the cost of calculation time. However, with ever increasing computing powers, this is not a big issue any more.

**i. LC-MS data pre-processing**—With all of the EICs built, feature detection determines all of the chromatographic peak features. A feature is defined as an ion with a unique combination of  $m/z$  and retention time values. In an EIC, there could be one or more chromatographic peak features. Since these peak features could be of different widths, wavelet transform has been used as a robust method for this purpose.

Among all of the peak features, a high percentage of them are produced by random noise and contaminants and need to be filtered out. A few criteria can be used for filtering, including the signal-to-noise ratio of each peak feature, the width, the shape, and total area underneath a feature. This is achieved in the step of feature filtering. Subsequently, all of the remaining peak features in a data file are grouped based on their chromatographic peak shape. Peaks that are similar in terms of the shape are most likely related to a single metabolite. These peaks in the same group could be isotopes, adducts, neutral-losses and the molecular ions<sup>8</sup>. What would eventually determine the identity of the molecule that has produced this group of ions is the molecular ion.

For each feature group, each feature is assigned a most likely ion type (isotope, adduct, neutral-loss, or molecular ion) in the feature annotation step.

So far, each processing step including mass recalibration, centroiding, feature detection, feature filtering, feature grouping, and feature annotation have been carried out for each data file. With all of the features that have been annotated for each data file, features are aligned across data files. The purpose of this step is to correct retention time shift that has occurred in the course of analyzing many biological samples on the analytical platforms.

Many retention time correction methods are used in existing software. A warping-based approach by modeling the global retention time shift over time finds similar peak shapes to warp the spectra to a median spectrum. Another is to find anchors, features that do not have a large drift in time. These anchors can then be used to align the LC-MS spectra in a non-linear fashion. A third is to determine features that correspond to the same metabolite across data files. The criteria for this determination include similarity in terms of isotopic profile, mass, and retention time. The latter approach is computationally more challenging and more time consuming, but more accurate.

Software(s) to perform the aforementioned is(are) provided by individual instrument manufacturers. However, there are extremely useful community providers of this type of software. A very powerful software for analysis of metabolomics data is XCMS<sup>6</sup>. It can be used on an investigator's computer at the command line level using R. Alternatively, investigators can upload their data to an online version of XCMS (<https://xcmsonline.scripps.edu>)<sup>9</sup>. Depending on the instrument generating their data, it may be necessary to convert the data into .mzML, .mzXML or .NetCDF format<sup>10</sup>. Once loaded, an investigator selects the individual datasets to be compared, adjusts certain parameters based on the nature of the GC-MS or LC-MS instrumentation (acceptable peak widths, mass

accuracy, etc.), and submits a job for the Scripps server to process. Once ready, the investigator reviews the results online. These come in graphical form (color-coded total ion current chromatograms with and without retention time warping, Cloud plots (Fig. 3) identifying ions that are increased (green) or decreased (red) superimposed on the mean total ion chromatogram (in gray), and multidimensional statistical plots<sup>11</sup>. Furthermore, a more interactive form of XCMSonline has become available<sup>12</sup>. The data can also be exported and after arranging into files containing  $m/z$  values of the ions and their intensities, can be analyzed by other statistical programs that are freely available on the internet. One of these is MetaboAnalyst ([www.metaboanalyst.ca](http://www.metaboanalyst.ca)). Metabolites can also be compared across different datasets using metaXCMS<sup>13</sup>.

A second publicly available program that in addition is excellent for data presentation is Mzmine<sup>14</sup> – it can be downloaded at <http://mzmine.github.io/> and works on both Macs and PCs. Once loaded, the user has the option of working at the command line and thereby writing programs to optimize use of Mzmine, or using a graphical user interface to utilize pre-programmed software functions. The file formats that can be used with Mzmine are .CDF and .mzXML. Once loaded, a useful way of looking at the MS data is to plot the intensities of either selected ion masses or ranges of ions masses for user-defined times. To assist in the identification of significant peaks, the ions can be displayed in a 3D-plot (Fig. 4A). In this example, the urine was from a subject who had been treated with gemcitabine. By selecting  $m/z$  264.08 with a 5 ppm mass window, an ion chromatogram revealed that gemcitabine eluted at 15.2 min (Fig. 4B). Mzmine has filtering functions for the raw data including carrying out alignment across multiple samples. There are other programs that can be used in this context and recently they have been evaluated comparatively<sup>15</sup>.

**ii. GC-MS data pre-processing**—A major difference between pre-processing LC-MS and GC-MS data is that the latter must include a deconvolution step for constructing a “pure” spectrum for each metabolite measured by the mass analyzer. This is because GC-MS analytical platforms usually use electron ionization that causes fragmentation of molecules at the ionization source. As a result, what the mass analyzers produce are fragmentation spectra, similar to the MS/MS spectra that are produced on LC-MS platforms. Since different metabolites could elute from the gas chromatography column at the same time (co-elution) when separation is not perfect, the same GC-MS spectrum could contain fragments from different metabolites and deconvolution is needed to separate them into their individual spectra.

For this purpose, AMDIS (Automated Mass Spectral Deconvolution and Identification) was developed and has been widely used (<http://chemdata.nist.gov/mass-spc/amdis/downloads/>).

### c. Statistical Analysis

With the quantitative information of metabolite ions (peak area or peak height) determined at the data pre-processing stage, statistical algorithms are applied to identify those ions that are significantly altered between control and experimental groups. Before statistical analysis can begin, it is necessary to remove from the file of integrated peak areas those from the dead volume before any of the sample reaches the mass spectrometry detector and those

eluting during column washing and re-equilibration. Selective removal of NMR peaks may also be carried out as noted above.

The fully processed data are then uploaded to MetaboAnalyst<sup>16</sup> ([www.metaboanalyst.ca](http://www.metaboanalyst.ca)). Data are organized into individual Excel files in the .csv format. The first column of each file is the list of  $m/z$  values or the list of <sup>1</sup>H-NMR chemical shifts. The second column is the corresponding peak area for each  $m/z$  value or NMR chemical shift. The files are organized in folders into the two groups being compared. Note that the names of each file and of the folders must not include spaces. The two folders are combined into a .zip file and uploaded to MetaboAnalyst (which will check for any errors and if none report on the total number of metabolites to be analyzed). MetaboAnalyst also checks for missing values and allows for selection of interquartile range (preferred). Next, it is important to apply a normalization function. Commonly this is a weighted correction to the collected data. This could very simply be due to differences in the amount of sample taken. For example, in a study involving collected plasma, all the samples except two had 100  $\mu$ L of plasma available. The volumes of the other two samples were 75  $\mu$ L and 90  $\mu$ L. The peak areas of the latter two sample dataset values were therefore increased by 100/75 and 100/90, respectively. As noted earlier, it is important to have internal standard(s) added to the samples being processed. A further correction to peak areas is then to normalize to the mean area of the standard across all samples divided by the area of the standard in individual samples.

While the above approach works for plasma and serum, fluids such as urine, follicular fluid and bronchoalveolar lavage are subject to dilution that it is a function of either how much an animal or human subject has drunk prior to collection (urine), or how much fluid (physiological saline) was flushed into a cavity to recover follicular fluid and bronchoalveolar lavage. In these cases, other correcting factors can be employed. For urine, the creatinine concentration has been widely used to do this correction although in cases of kidney dysfunction it is not appropriate. For follicular fluid and bronchoalveolar lavage with unknown dilutions caused by the lavage fluid, normalization by dividing by the total ion current (TIC) is a reasonable approach. The assumption here is that the greater majority of the observed signals are unchanged and therefore the sum of the observed ions is an effective normalizing factor.

The next consideration for the dataset is to apply the interquartile range (IQR). If all the data are ranked and divided into four equal parts, the IQR represents the middle 50% of all the data points. If the data are not normally distributed, then log transformation may be applied although this creates problems since it cannot handle zero values. Finally, to reduce the contribution of the most intense ions in the dataset, the data can be mean centered (i.e., the mean value for a metabolite is subtracted from each metabolite ion value) and then the variance is scaled by the square root of the standard deviation. The data are now ready for univariate and/or multivariate analysis<sup>16</sup>.

Many different normalization functions have been developed and are suitable to different problems including both dilution and batch effects<sup>16, 17</sup>. Median fold change normalization has the ability to reduce dilution effects without altering the biological effect. This method



was tested with log transformations of LC-MS data and showed to improve overall analysis with multivariate statistics by increasing the statistical agreement with these methods.

**i. Univariate analysis**—A serious problem encountered in applying statistical analysis to all -omics data is that the number of samples ( $n = 3-6$  for cells,  $n = 8-15$  for an animal study,  $n = 30-100$  for a controlled clinical study and  $n = 100-1,000$  for an epidemiological study) is smaller than the number of observed variables. Taking a univariate approach, a Student's t-test comparing the amount of a single metabolite ion in a control group with another in a treatment group and selecting significant metabolites based on p-values is fraught with problems due to the multiple testing issue. The Bonferroni correction<sup>19</sup>, dividing the normally acceptable p-value for significance for comparison of a variable between two groups ( $p < 0.05$ ) by the number of observed metabolite ions ( $m$ ) is very harsh and may result in the loss of real metabolite differences. Using fold-change as a discriminator, as was widely used in the early days of transcriptomics<sup>20</sup>, is no longer regarded as acceptable. However, the use of a Volcano plot (Fig. 5) that combines fold change and pairwise significance is widely accepted<sup>21</sup>. In this, fold-change is plotted as the logarithm to the base two on the horizontal axis and the negative logarithm of the p-value on the vertical axis. The investigator may select a reasonable fold-change, say 1.5, and p-value, say  $p < 0.01$  ( $\log_{10} P = 2$ ). In the plot, metabolites appearing in the upper left and right quadrants are considered candidates for metabolites which are significantly changed. The false discovery rate (FDR) correction of the p value (resulting in a q value) is becoming a widely accepted alternative to the Bonferroni correction<sup>22, 23</sup>. This method is a less stringent, multiple testing correction that results in fewer features/metabolites as false negatives. There are many variations of the FDR approach and their variability in output has been systematically evaluated<sup>24</sup>.

**ii. Multivariate analysis**—The data may also be analyzed using multivariate analysis. The two major methods currently used in the field are principal components analysis (PCA) and partial least squares discriminant analysis (PLS-DA). PCA is a data reduction technique that allows high dimensional datasets (such as those in metabolomics) to be reduced to a few major principal components. By plotting the scores (the weighted sum of the contribution of each metabolite to a principal component) of these components (normally principal components with eigen values greater than 1), users may find that a class of observations (samples) are distinct from one another (Fig. 6A). Using the loadings plot features that are contributing to this separation, metabolite ions can be selected and further analyzed to identify if they are biologically relevant metabolites. It should be noted that as PCA does not use any data classification to find the principal components, it is a non-supervised method. The other major method, PLS-DA, is a supervised method. This method uses a binary class group (Y) to explain the variables in the data matrix (X). Much like PCA, PLS-DA scores plots can be viewed with different projections in the scores and loadings plots (Fig. 7). Simca (<http://www.umetrics.com/products/simca>), a well-used multivariate software analysis suite, and MetaboAnalyst<sup>16</sup> output the variable importance in projection (VIP) score. This score can be used along with a contribution score to find the most predictive features for the class.

By selecting those metabolites that appear to be significant in both univariate and multivariate analysis, there is an increased chance that they can be validated in separate experiments. It is necessary then to look at selected ion chromatograms for these metabolite  $m/z$  values to eliminate any metabolites that have irregular peak shapes. Also, it is also worth filtering the results to isolate for further analysis those peaks that had sufficient intensity to trigger collection of MS/MS data.

#### d. Confirming metabolite data

Even a metabolite ion that is strongly related to the phenotype being studied and has shown to be significantly different by univariate and/or multivariate analysis must be confirmed by independent LC-MS analysis. Typically, the mass transitions between the precursor ions (MS1) and their product ion(s) formed by MS/MS (that were collected in untargeted metabolomics analysis) are used to generate a multiple reaction monitoring assay. Ideally, this assay is carried out on sets of biological samples held back from the untargeted metabolomics analysis so as to provide an independent assessment of the significance of the metabolites.

**i. Identifying metabolite ions**—Once statistical analysis has generated a list of potentially changed metabolite ions, their  $m/z$  values can be matched against public metabolite databases such as METLIN (<https://metlin.scripps.edu/index.php>), the Human Metabolite Database (<http://www.hmdb.ca>), and the Lipidmaps database (<http://www.lipidmaps.org>). These databases contain MS and MS/MS information. A disadvantage that investigators frequently encounter is that the databases contain different sets of metabolites and when metabolites are in common, the databases use different alphanumeric IDs. In addition, there are proprietary databases as part of workstations (MassHunter) associated with commercial instruments (Agilent), as well as those in comprehensive metabolomics analysis services such as Metabolon (<http://www.metabolon.com>). The Fiehn lab provides a tool for interconversion of metabolite IDs (<http://cts.fiehnlab.ucdavis.edu>). Although it interconverts IDs from a very long list of databases, at the present time it is not possible to convert METLIN IDs to other formats. It is also common that investigators do not find their feature in a database either because the feature is not a metabolite, the feature is an adduct and is not being searched correctly in the database, or the metabolite is not in the databases yet.

For GC-MS data, the Fiehn lab (<http://metabolomics.ucdavis.edu>) and the NIST databases (<http://www.nist.gov/srd/nist1a.cfm>) provide extensive searching capabilities.

Besides the biochemical databases, there are others that are more comprehensive, encompassing all known chemicals. One of these is Chempider (<http://chemspider.com>). By entering the monoisotopic mass (note, not the mass of the ion, but the molecular weight of the unionized molecule) under *intrinsic properties*, all records with that mass can be downloaded. For instance, the isoflavone genistein with empirical formula  $C_{15}H_{10}O_5$  has a monoisotopic mass of 270.053 Da. If the mass window is limited to  $\pm 0.01$  Da, there are 3,316 records in Chempider, although not all the compounds retrieved have the formula  $C_{15}H_{10}O_5$ . Narrowing the mass window ten-fold to  $\pm 0.001$  Da reduces the number of



records to 319; however, every one of them has the empirical formula  $C_{15}H_{10}O_5$ . Therefore, no matter how powerful a mass spectrometer may be at determining *exact mass*<sup>2</sup>, it is likely that there are multiple other (isobaric) compounds at that mass.

A comprehensive analysis of an unknown metabolite in terms of its LC or GC retention time, isotope distribution, accurate mass, and fragment ion patterns in MS/MS helps to identify its structure.

Exact mass does have an advantage in that it may allow the investigator to determine the empirical formula of a metabolite. Because the mass defects for each element (except carbon) are non-zero, observed masses do not form a continuum of masses. Metabolites that are fully saturated with hydrogen have the highest, positive mass defect. For instance, the monoisotopic ion of palmitate  $[M-H]^-$  molecular ion is  $m/z$  255.233 with its 31 hydrogens each contributing 0.00783 Da to the mass defect. On the other hand, the monoisotopic mass of the  $[M-H]^-$  ion of 5-methylthio-D-ribose-1-phosphate (empirical formula  $C_6H_{12}O_7PS$ ) is 259.004. The small mass defect for this metabolite occurs because the negative mass defects of seven oxygen atoms (each  $-0.00509$  Da), phosphorus ( $-0.02624$  Da) and sulfur ( $-0.02793$  Da) offset the positive mass defect of the 12 hydrogen atoms.

Of course, chromatographic retention time is an additional, independent parameter to be used in confirming or denying metabolite identity. Indeed, investigators use (at least) two different LC methods to ensure identity. Usually, this involves different stationary phases (e.g., reverse-phase versus hydrophilic interaction liquid chromatography) or mobile phases with different pHs, e.g., 0.1% formic acid (pH 2) and 10 mM ammonium acetate (pH 7). Where the metabolite has a chiral center (and thereby the R- and S-isomers otherwise behave identically), a chiral stationary phase may have to be employed. Ion mobility mass spectrometry is a powerful approach for the study of metabolites<sup>25</sup> and has recently been applied to the separation of isomeric, isobaric lipid metabolites<sup>26</sup>.

**ii. Interpreting MS/MS data**—While identifying metabolite ions may eventually be computer-driven, at the present time less than 20% of the observed ions (at exact masses) have putative identities. Of those that have an ascribed chemical identity, only an even smaller number have associated MS/MS spectra. A complication in interpreting MS/MS spectra is that the product ions and their ratios that are observed are in part due to the mass spectrometer being used and the conditions for collision-induced dissociation. MS/MS spectra in the METLIN database are recorded at increasing potential gradients (0, 10, 20 and 40 V) giving successively greater extents of ion dissociation. In real time LC-MS analysis, many systems use a rolling potential during analysis of a selected peak since it cannot be predicted *a priori* what the optimum potential is for dissociation of an unknown precursor ion. This thereby leads to a MS/MS spectrum that is an average.

As such, interpreting MS/MS spectra may involve not only comparison to MS/MS spectra of precursor ions of the same  $m/z$  as the metabolite, but also to other precursor ions with

---

<sup>2</sup>Exact mass is correct in the sense that a compound has an exact mass. However, experimental measurement of the mass of an ion always has error. The most accurate mass spectrometers used in metabolomics can measure mass with an error of  $\sim 100$  ppb, i.e., to the 5<sup>th</sup> decimal place.

different  $m/z$  values where the product ions are nonetheless the same. This suggests that metabolite and the known compound are structurally similar<sup>27, 28</sup>.

Direct comparisons between product ions of standards and unknowns can provide important structural information of unknown biological products. For example, 3'-chlorodaidzein was identified when differentiated HL-60 cells were incubated with the isoflavone daidzein (7,4'-dihydroxyisoflavone). Its identification was based on comparison between the product ion mass spectra of the standard and the biological product (Fig. 8A, B). The presence of the  $m/z$  35 ion together with the loss of 36 Da (HCl) indicated that daidzein had been chlorinated<sup>29, 30</sup>. Isomers such as C- and O-glucosides of flavonoids can be distinguished by their MS/MS fragmentation patterns<sup>31</sup>. For example, the carbon-carbon link in the C-glucoside of daidzein (puerarin) is relatively stronger than the ether linked O-glucoside (daidzin). For daidzin, ions break easily at the weakest point and the entire sugar moiety in daidzein 7-O- $\beta$ -D -glucoside is lost (-162 Da) (Fig. 8C). In contrast, for the C-glucoside puerarin, the glucose moiety is retained and ions representing losses of water are prominent (Fig. 8D).

Interpreting MS/MS data is also very useful in studying metabolic transformation. For example, the loss of glucuronic acid (176 Da) can be used for the characterization of  $\beta$ -glucuronide metabolites observed in serum/plasma, urine and other biofluids<sup>32</sup>. Similarly, GSH conjugates upon MS/MS produce characteristic product ions  $m/z$  306, 272, 254, 210, 179, 160 and 143 in the negative ion mode<sup>33</sup>.

Other methods used to discern the identity of a metabolite are similar to compound identification in natural products chemistry. These methods begin with preparative chromatography to isolate the metabolite in increasingly more purified forms. This allows both chemical derivatization to identify the number and nature of reactive groups and chemical or enzymatic hydrolysis to examine the conjugate nature of the metabolite. If very pure forms of the metabolite can be obtained, other spectroscopic methods can be brought into the analysis. These include infra-red analysis as well as NMR. If enough of the metabolite is isolated, NMR is particularly valuable since pulse sequence methods can be used to determine the protons attached to individual carbon atoms, and those protons that are interacting and the distances between them. This information is critical to differentiate between compounds based on GC-MS or LC-MS information.

**iii. Use of isotopes in metabolite analysis**—Isotopic labeling of precursors to identify metabolites in a pathway has had a history of more than 80 years. It began with deuterated water and moved onto the use of <sup>3</sup>H and <sup>14</sup>C radiolabeled forms of metabolite precursors. To enable studies in humans, emphasis has been placed on the use of stable isotopes (<sup>2</sup>H, <sup>13</sup>C, <sup>15</sup>N and <sup>18</sup>O). By starting with uniformly <sup>13</sup>C-labelled glucose, all the metabolites that constitute primary and secondary pathways of its metabolism can be discerned by following the increased <sup>13</sup>C-intensities of the metabolites. Both NMR and mass spectroscopic methods are widely used in stable isotope resolved metabolomics analysis.

An interesting development to these methods is IROA (isotope ratio outlier analysis, <http://www.iroa.com>)<sup>34</sup>. In this method two forms of <sup>13</sup>C-labeled glucose are incubated with the

system under test. The first form is 95%  $^{13}\text{C}/5\%$   $^{12}\text{C}$ -glucose (experimental condition) and the other is 5%  $^{13}\text{C}/95\%$   $^{12}\text{C}$ -glucose (control condition). When extracts of each are mixed, ions representing metabolites have a U-shaped isotope profile - the extremes are all  $^{12}\text{C}$ -labeled and all  $^{13}\text{C}$ -labeled forms of the metabolite. Usefully, the difference in mass between the all  $^{12}\text{C}$ -labeled and all  $^{13}\text{C}$ -labeled forms of the metabolite represents the number of carbon atoms it has (Fig. 9). This can be very valuable in limiting the number of empirical formulae that are consistent with the observed  $m/z$  of the metabolite. A similar approach (HiTIME, High-Resolution Twin-Ion Metabolite Extraction) has been described for the metabolites of acetaminophen<sup>35</sup>.

As a final step, it's typical to chemically synthesize the new metabolite, either to verify that it is identical to the biological metabolite, or to use it in an isotopically labeled form for pathway analysis or absolute quantitation by isotope dilution mass spectrometry analysis. The NIH Common Fund Metabolomics Program has issued contracts to RTI International and SRI International for metabolite synthesis. Interested investigators may nominate compounds for synthesis or request existing compounds at <http://www.metabolomicsworkbench.org/standards/nominatecompounds.cgi>.

## 2. Pathway analysis

Metabolomics has two principal goals: to identify (1) a useful biomarker or panel of biomarkers that accurately predict a particular phenotype, and/or (2) the metabolic pathway(s) and hence the underlying proteins and/or genes that lead to the phenotype. Whereas biomarkers, once validated, allow immediate implementation, knowledge of pathways may allow targeting of an enzyme activity, a transporter of a metabolite, or a transcription factor regulating a metabolic process. Many of the biochemical pathways were established in the early days of biomedical research once isotopically labeled forms of metabolite precursors became available. Databases of these pathways and more recently described pathways are available in publicly accessible and searchable sites such as KEGG (Kyoto Encyclopedia of Genes and Genomes - <http://www.genome.jp/kegg/>), MetaCyc (<http://metacyc.org>), BioCyc (<http://biocyc.org>) and Metscape (<http://metscape.ncibi.org/>) which is a plug-in for Cytoscape (<http://cytoscape.org>). GeneGo (<https://portal.genego.com/>) and Ingenuity pathway analysis (<http://www.ingenuity.com/products/ipa>) are examples of commercial pathway analysis software tools.

A novel approach to connecting metabolites is Mummichog (<http://mummichog.org>). It started as a pathway and network analysis tool for untargeted metabolomics<sup>36</sup>. Mummichog assumes that statistical testing at feature level, even without metabolite annotation, can select a subset of  $m/z$  features that carry biological meanings, which can be potentially projected onto metabolic networks as enriched patterns (Fig. 10). Such patterns can be quantified by over-representation statistics, in combination with network topologies. The null distribution is estimated by resampling all  $m/z$  features, and multiple matches between  $m/z$  and metabolites are taken into account. Both conventional pathways and unbiased network analysis are accommodated in this framework. Thus, Mummichog can quickly generate high-quality hypotheses from untargeted data, so that researchers can focus their resources

on prioritized pathways and biological context. This approach can be successfully applied to mechanistic experiments<sup>37</sup> and population-based studies<sup>38</sup>.

A deeper appreciation of the role of the microbiome that has also occurred in recent years has led to the realization that metabolism crosses genomic boundaries. Because the human is now described as a superorganism<sup>39</sup>, a combination of human eukaryotic cells and the prokaryotes inhabiting the gastrointestinal tract in vast numbers and those in other crevices, this must be taken into effect when considering metabolites and the metabolic pathways they are associated with. In addition, metabolites arise from the foods we eat, often another discrete set of genomes.

For example (Fig. 11), the isoflavone daidzein is found in the soybean mostly as its 6''-O-malonyl-7- $\beta$ -D-glucoside<sup>40</sup>. Traditional preparation of soy foods either by hot water extraction (to make soy milk and tofu) largely leads to hydrolysis of the malonate group to yield the 7- $\beta$ -D-glucoside of daidzein<sup>41</sup>. Fermentation of soy to make miso, soy paste or tempeh causes hydrolysis all the way to daidzein as well as to the introduction of hydroxyl groups. Many American soy foods are based on the protein fraction of soy once the oil, but not the isoflavones, has been removed by extraction. Processing of the protein fraction using heat causes decarboxylation of the malonyl group to form 6''-O-acetyl-7- $\beta$ -D-glucoside of daidzein<sup>41</sup>. Note that these steps do not represent metabolism, but instead a chemical (processing) pathway. Once in the gastrointestinal tract, daidzein, as for other isoflavones<sup>42</sup>, is easily absorbed into the intestinal cells. The 7- $\beta$ -D-glucoside of daidzein which may enter the intestinal cell via the glucose transporters undergoes hydrolysis catalyzed by lactase phloridzin hydrolase<sup>43</sup>. In the intestinal cell, daidzein is mostly converted to its  $\beta$ -glucuronide<sup>42</sup> or sulfate ester. These phase II metabolites enter the bloodstream and are swept towards the liver where they undergo hepatobiliary transport from the portal vein into the bile. The  $\beta$ -glucuronide, 6''-O-malonyl-7- $\beta$ -D-glucoside and 6''-O-acetyl-7- $\beta$ -D-glucoside of daidzein are not substrates of lactase phloridzin hydrolase and therefore enter the microorganism-rich colon. The bacteria there hydrolyze each of these conjugates to daidzein which undergoes reductive metabolism to form dihydrodaidzein, O-desmethyldaidzein and equol (4,7-dihydroxyflavan). Whereas daidzein has no chiral carbon atoms, its metabolites have a C<sub>3</sub> asymmetric carbon. It has been shown that the naturally occurring form of daidzein is its S-isomer<sup>44</sup> which binds to estrogen receptor with a K<sub>D</sub> of 1 nM, similar to 17 $\beta$ -estradiol (the R-isomer, made chemically, is a weak agonist). These metabolites are absorbed from the colon, return to the liver via the inferior mesenteric drainage and are glucuronidated and re-enter the bile. This set of metabolic steps between the daidzein in soy foods and S-equol therefore crosses three different types of genomes (Fig. 11) and at this time is not represented in pathway databases.

### 3. Fluxomics analysis

The concentrations of metabolites, even when measured accurately and precisely, give no sense of the dynamic nature of metabolism or the origins of the carbon atoms (and when appropriate nitrogen atoms) in a metabolite. The concentrations and turnover of metabolites sitting at the junctions of metabolic pathways such as pyruvate, acetyl CoA, alpha-ketoglutarate, glutamate and glutamine may reveal the underlying features of disease<sup>45</sup>. To

pursue this area of metabolomics it is necessary to combine both high performance GC-MS or LC-MS and NMR<sup>46–50</sup>. LC-MS is used to determine the concentrations of each metabolite and <sup>13</sup>C-NMR allows the identification of which carbon atoms are <sup>13</sup>C-labeled and to what extent.

#### 4. Imaging-MS

Although much of the reported information in metabolomics concerns biofluids, there is a growing interest in the location of metabolites in tissues. Although secondary ion mass spectrometry (SIMS) has been used to examine intracellular metabolites<sup>51</sup>, two main approaches are currently being used: rapid evaporative ionization mass spectrometry (REIMS) that exploits analysis of the sprays created by the surgeon's cauterizing knife<sup>52–54</sup>, and imaging of frozen tissue sections using direct electrospray ionization (DESI)<sup>55–57</sup> or MALDI-imaging MS<sup>58, 59</sup>. In the latter case it is necessary to deposit the MALDI matrix by vacuum sublimation in order to prevent shifting of the metabolites and to ensure optimum matrix deposition. This limits the available matrices to those that undergo sublimation. Using 2,5-dihydrobenzoic acid (DHB) as a matrix applied to frozen tissue sections by vacuum sublimation, the major lipids that are altered quantitatively in normal processes such as ageing or in disease processes can be viewed spatially. This information helps to establish mechanism and suggests possible physiological consequences of those lipid changes. An example from our group<sup>60</sup> is shown in Figure 12. Several ether-linked phospholipids were found to be increased early after ischemia-reperfusion kidney injury in mice using MS/MS<sup>ALL</sup> lipidomics. One of these was imaged using 2,5-DHB matrix coated kidney cryosections in positive mode to show that it was located primarily to regions of the kidney rich in proximal tubules. In MALDI imaging, TOF<sup>58</sup> and TOF/TOF analyzers are most frequently used<sup>59, 61</sup>, although higher mass resolution can be obtained with FT-ICR analyzers<sup>62</sup>. Whereas SIMS using heavy ion bombardment can provide subcellular spatial resolution (50 nm), the spatial resolution using MALDI is limited to the width of the beam (5–25 μm).

#### 5. Further training opportunities

Besides the UAB Metabolomics workshop, there are several metabolomics symposia and associated short workshops at institutions sponsored by the NIH Common Fund Program in Metabolomics (RTI International, University of Florida, University of Michigan and the Mayo Clinic), as well as advanced workshops at UC-Davis (advanced data processing) and the University of Kentucky (fluxomics and stable isotopes). There are many international workshops and a calendar of these is presented monthly in MetaboNews (<http://www.metabonews.ca/archive.html>). There are a growing number of workshops given in conjunction with meetings of National Societies. The Metabolomics Society (<http://metabolomicsociety.org>) has annual international meetings and has developed a subgroup for young investigators.

## 6. The future of metabolomics

Standardization of methodology and advancement in technology will enable the use of simpler systems to more easily extract, measure, and quantify the metabolome. As untargeted approaches reveal relevant metabolites for a system, more focused, targeted assays can then be used to validate these studies. As an example, a recent study used the available isotopically labeled metabolite standards to measure quantitatively more than 100 metabolites at a time using triple quadrupole MRM-MS<sup>63, 64</sup>. It should be expected that in the future commercial companies will develop kits for the quantitative analysis of specific classes of metabolites in which every metabolite to be measured can be added to the extraction solvent in a stable, isotopically-labeled form. This isotope dilution approach will allow the collection of quantitatively reliable metabolite data that could be compared across different investigator groups, enhancing the value of these data and permitting their integration with other –Omics data.

With analyzers that allow 200 mass transitions to be monitored per second, analysis with peaks that are 10 s wide are currently available. With faster switching between transitions and more sensitive detection of metabolite ions, further improvements will occur. How many product ions are needed to successfully discriminate between metabolites has been approached bioinformatically<sup>65</sup>. However, since it will take many product ions to do this, this redundancy noticeably increases the number of mass transitions to monitor and hence consumes time. Q-TOF mass spectrometers provide an alternative avenue for improvement since they can also be used to carry out MRM analysis with the advantage that they collect all the product ions of a selected precursor ion at one time and with much greater accuracy than a quadrupole detector<sup>63</sup>.

With very fast analyzers like the TOFs, it is also possible to generate massively parallel separations, such as those possible with capillary electrophoresis. In addition, high-resolution chromatography using a combination of open-tubular and packed on chips operating in nanofluidics is emerging as a future device<sup>66</sup>.

In the future, software for processing metabolomics data and identifying metabolites may move into the Cloud. The advantage of doing this is that the high current, upfront expense of standalone software (>\$35,000) and computer hardware adequate to run the programs (>\$5,000) can be avoided. Although use of the software may require a subscription service, it would allow users to (a) work with the latest version of the software, (b) employ as many virtual computers as needed for the job in hand and (c) integrate this form of –omics data with data from all the other –omics. Of course, legal and proprietary issues may limit this approach. At this time, individual institutions may interpret Health Insurance Portability and Accountability Act (HIPAA) regulations regarding patient privacy to prevent the use of the Cloud for data processing/data storage. For similar reasons companies may not wish to put sensitive information in the Cloud. On the other hand, NIH and other federal agencies demand that data obtained with public funds be placed in databases accessible to interested parties. The value of putting the software in the Cloud will be to encourage all investigators to take part in a community development of the software. Another advantage of going to the Cloud is that it would allow the combination of metabolomics data with genomics,



transcriptomics and proteomics data. Until recently, inconsistencies in formatting between the data domains made this impossible on the large scale. However, SCIEX is developing a OneOmics capability with the Illumina in the Amazon Cloud (<http://sciex.com/solutions/life-science-research/multi-omics-bioinformatics>). This should allow the integration of the massive amounts of –Omics data and greatly facilitate discovery of the underlying bases of diseases as well as the aging process.

All of these developments would be similar to the transition that occurred from refrigerator-sized computers with 8k of memory in the 1960s to 50 years later with hand-carried, smart phones with 64 GB of memory. However, to do so will require continuing investment in physics and the rest of science and a demonstrated value of measuring the metabolome.

Finally, integration of data from the metabolomics, genomics and transcriptomics domains is a long sought-after goal of the investments in biomedical research and will certainly support the implementation of personalized (and accurate) medicine.

## Acknowledgments

Funds for the National Workshop in Metabolomics came from NIH grant R25 GM103798-03. The workshop also received support from the UAB Office of the Vice-President for Research and Economic Development, the UAB School of Medicine and College of Arts and Science, the UAB Comprehensive Cancer Center (P30 CA13148), the UAB Comprehensive Diabetes Center, the UAB Diabetes Research Center (P60 DK079626), the UAB Center for Free Radical Biology, and the UAB-UCSD O'Brien Center for Acute Kidney Disease (P30 DK079337), and the Departments of Chemistry and Pharmacology and Toxicology. We are also grateful for unrestricted support from Metabolon, Sciex and Waters. Acknowledgements are also given to Dr. N. Rama Krishna for the use of the Central Alabama NMR facility and to staff who assisted in the running of the workshop (UAB: Jennifer Spears, Lynn Waddell, Mikako Kawai, D. Ray Moore II, Landon Wilson, Ali Arabshahi, and Ronald Shin; RTI International, Rodney Snyder) and student trainees, Haley Albright, Kelly Walters and Sean Wilkinson. We are indebted to faculty who have also previously contributed to the development of the workshop: Dr. Kathleen Stringer (University of Michigan), Dr. Dean P. Jones (Emory University), Dr. Grier P. Page (RTI International), Dr. Olga Ilkayeva (Duke University), Dr. Nikolaos Psychogios (Shire Pharmaceuticals) and Dr. Natalie Serkova (University of Colorado-Denver) and to faculty in receipt of NIH Administrative Supplements (Dr. Lalita Shevde-Sumant, R01 CA138850 and Dr. Adam Wende R00 HL111322). Finally, the workshop has been enhanced by several plenary speakers: Dr. Stanley Hazen (Cleveland Clinic), Dr. Keith Baggerly (MD-Anderson), Dr. Richard Caprioli (Vanderbilt University), Dr. Arthur Edison (University of Florida) and Dr. David Wishart (University of Alberta), as well as speakers from several companies: Brigitte Simons and Jeremiah Tipton (SCIEX), Tom Beatty and John Shockcor (Waters) and Edward Karoly and Rob Mohny (Metabolon).

## References

1. Barnes S, Benton HP, Casazza K, Cooper S, Cui X, Du X, Engler J, Kabarowski JH, Li S, Pathmasiri W, Prasain JK, Renfrow MB, Tiwari HK. Training in metabolomics research. I. Designing the experiment, collecting and extracting samples and generating metabolomics data. *J Mass Spec.* 2016 xx, yyy.
2. Eriksson L, Antti H, Gottfries J, Holmes E, Johansson E, Lindgren F, Long I, Lundstedt T, Trygg J, Wold S. Using chemometrics for navigating in the large data sets of genomics, proteomics, and metabonomics (gpm). *Anal Bioanal Chem.* 2004; 380:419. [PubMed: 15448969]
3. Trygg T, Holmes E, Lundstedt T. Chemometrics in metabonomics. *J Proteome Res.* 2007; 6:469. [PubMed: 17269704]
4. Savorani F, Tomasi G, Engelsen SB. icoshift: A versatile tool for the rapid alignment of 1D NMR spectra. *J Magn Reson.* 2010; 202:190. [PubMed: 20004603]
5. Veselkov KA, Lindon JC, Ebbels TMD, Crockford D, Volynkin VV, Holmes E, Davies DB, Nicholson JK. Recursive segment-wise peak alignment of biological  $^1\text{H}$  NMR spectra for improved metabolic biomarker recovery. *Anal Chem.* 2009; 81:56. [PubMed: 19049366]

6. Smith C, Want EJ, O'Maille G, Abagyan R, Siuzdak GE. XCMS: Processing mass spectrometry data for metabolite profiling using nonlinear peak alignment, matching, and identification. *Anal Chem.* 2006; 78:779. [PubMed: 16448051]
7. Tautenhahn R, Böttcher C, Neumann S. Highly sensitive feature detection for high resolution LC/MS. *BMC Bioinformatics.* 2008; 28:504.
8. Nordström A, O'Maille G, Qin C, Siuzdak G. Nonlinear data alignment for UPLC-MS and HPLC-MS based metabolomics: quantitative analysis of endogenous and exogenous metabolites in human serum. *Anal Chem.* 2006; 78:3289. [PubMed: 16689529]
9. Tautenhahn R, Patti GJ, Rinehart D, Siuzdak G. XCMS Online: a web-based platform to process untargeted metabolomic data. *Anal Chem.* 2012; 84:5035. [PubMed: 22533540]
10. Martens L, Chambers M, Sturm M, Kessner D, Levander F, Shofstahl J, Tang WH, Römpp A, Neumann S, Pizarro AD, Montecchi-Palazzi L, Tasman N, Coleman M, Reisinger F, Souida P, Hermjakob H, Binz PA, Deutsch EW. mzML--a community standard for mass spectrometry data. *Mol Cell Proteomics.* 2011; 10:R110.000133.
11. Patti GJ, Tautenhahn R, Rinehart D, Cho K, Shriver LP, Manchester M, Nikolskiy I, Johnson CH, Mahieu NG, Siuzdak G. A view from above: cloud plots to visualize global metabolomic data. *Anal Chem.* 2013; 85:798. [PubMed: 23206250]
12. Gowda H, Ivanisevic J, Johnson CH, Kurczy ME, Benton HP, Rinehart D, Nguyen T, Ray J, Kuehl J, Arevalo B, Westenskow PD, Wang J, Arkin AP, Deutschbauer AM, Patti GJ, Siuzdak G. Interactive XCMS Online: simplifying advanced metabolomic data processing and subsequent statistical analyses. *Anal Chem.* 2014; 86:6931. [PubMed: 24934772]
13. Tautenhahn R, Patti GJ, Kalisiak E, Miyamoto T, Schmidt M, Lo FY, McBee J, Baliga NS, Siuzdak G. metaXCMS: second-order analysis of untargeted metabolomics data. *Anal Chem.* 2011; 83:696. [PubMed: 21174458]
14. Pluskal T, Castillo S, Villar-Briones A, Oresic M. MZmine 2: modular framework for processing, visualizing, and analyzing mass spectrometry-based molecular profile data. *BMC Bioinformatics.* 2010; 11:395. [PubMed: 20650010]
15. Niu W, Knight E, Xia Q, McGarvey BD. Comparative evaluation of eight software programs for alignment of gas chromatography-mass spectrometry chromatograms in metabolomics experiments. *J Chromatogr A.* 2014; 1374:199. [PubMed: 25435458]
16. Xia J, Sinelnikov IV, Han B, Wishart DS. MetaboAnalyst 3.0-making metabolomics more meaningful. *Nucleic Acids Res.* 2015; 43:W251. [PubMed: 25897128]
17. Veselkov KA, Vingara LK, Masson P, Robinette SL, Want E, Li JV, Barton RH, Boursier-Neyret C, Walther B, Ebbels TM, Pelczar I, Holmes E, Lindon JC, Nicholson JK. Optimized preprocessing of ultra-performance liquid chromatography/mass spectrometry urinary metabolic profiles for improved information recovery. *Anal Chem.* 2011; 83:5864. [PubMed: 21526840]
18. Fernández-Albert F, Llorach R, Garcia-Aloy M, Ziyatdinov A, Andres-Lacueva C, Perera A. Intensity drift removal in LC/MS metabolomics by common variance compensation. *Bioinformatics.* 2014; 30:2899. [PubMed: 24990606]
19. Bonferroni CE. Teoria statistica delle classi e calcolo delle probabilità. *Pubblcazioni del R Istituto Superiore di Scienze Economiche e Commerciali di Firenze.* 1936; 8:3.
20. Schena M, Shalon D, Heller R, Chai A, Brown PO, Davis RW. Parallel human genome analysis: microarray-based expression monitoring of 1000 genes. *Proc Natl Acad Sci USA.* 1996; 93:10614. [PubMed: 8855227]
21. Jin W, Riley RM, Wolfinger RD, White KP, Passador-Gurgel G, Gibson G. The contributions of sex, genotype and age to transcriptional variance in *Drosophila melanogaster*. *Nat Genet.* 2001; 29:389. [PubMed: 11726925]
22. Benjamini Y, Drai D, Elmer G, Kafkafi N, Golani I. Controlling the false discovery rate in behavior genetics research. *Behav Brain Res.* 2001; 125:279. [PubMed: 11682119]
23. Storey JD. A direct approach to false discovery rates. *J Royal Stat Soc: Series B (Stat Meth).* 2002; 64:479.
24. Gadbury GL, Xiang Q, Yang L, Barnes S, Page GP, Allison DB. Evaluating statistical methods using plasmode data sets in the age of massive public databases: an illustration using false discovery rates. *PLoS Genet.* 2008; 4:e1000098. [PubMed: 18566659]

25. Kaplan K, Dwivedi P, Davidson S, Yang Q, Tso P, Siems W, Hill HH Jr. Monitoring dynamic changes in lymph metabolome of fasting and fed rats by electrospray ionization-ion mobility mass spectrometry (ESI-IMMS). *Anal Chem.* 2009; 81:7944. [PubMed: 19788315]
26. Damen CW, Isaac G, Langridge J, Hankemeier T, Vreeken RJ. Enhanced lipid isomer separation in human plasma using reversed-phase UPLC with ion-mobility/high-resolution MS detection. *J Lipid Res.* 2014; 55:1772. [PubMed: 24891331]
27. Gerlich MI, Neumann S. MetFusion: integration of compound identification strategies. *J Mass Spectrom.* 2013; 48:291. [PubMed: 23494783]
28. Allen F, Pon A A, Wilson M, Greiner R, Wishart DS. CFM-ID: a web server for annotation, spectrum prediction and metabolite identification from tandem mass spectra. *Nucleic Acids Res.* 2014; 42:W94. [PubMed: 24895432]
29. Prasain JK, Patel RP, Kirk M, Wilson LS, Botting N, Darley-USmar VM, Barnes S. Mass spectrometric methods for the analysis of chlorinated and nitrated isoflavonoids: a novel class of biological metabolites. *J Mass Spectrom.* 2003; 38:764. [PubMed: 12898656]
30. Boersma BJ, D'Alessandro T, Benton MR, Kirk M, Wilson LS, Prasain JK, Botting NP, Barnes S, Darley-USmar VM, Patel RP. Neutrophil myeloperoxidase chlorinates and nitrates soy isoflavones and enhances their antioxidant properties. *Free Radic Biol Med.* 2003; 35:1417. [PubMed: 14642389]
31. Prasain JK, Jones K, Kirk M, Wilson LS, Smith-Johnson M, Weaver C, Barnes S. Profiling and quantification of isoflavonoids in kudzu dietary supplements by high-performance liquid chromatography and electrospray ionization tandem mass spectrometry. *J Agric Food Chem.* 2003; 51:4213. [PubMed: 12848487]
32. Draper WM, Brown FR, Bethem R, Miille MJ. Thermospray mass spectrometry and tandem mass spectrometry of polar, urinary metabolites and metabolic conjugates. *Biomed Environ Mass Spectrom.* 1989; 18:767. [PubMed: 2790262]
33. Zhu X, Hayashi M, Subramanian R. Enhanced detection and characterization of glutathione-trapped reactive metabolites by pseudo-MS(3) transition using a linear ion trap mass spectrometer. *Chem Res Toxicol.* 2012; 25:1839. [PubMed: 22920186]
34. Edison AS, Clendinen CS, Ajredini R, Beecher C, Ponce FV, Stupp GS. Metabolomics and Natural-Products Strategies to Study Chemical Ecology in Nematodes. *Integr Comp Biol.* 2015; 55:478. [PubMed: 26141866]
35. Leeming MG, Isaac AP, Pope BJ, Cranswick N, Wright CE, Ziogas J, O'Hair RA, Donald WA. High-resolution twin-ion metabolite extraction (HiTIME) mass spectrometry: nontargeted detection of unknown drug metabolites by isotope labeling, liquid chromatography mass spectrometry, and automated high-performance computing. *Anal Chem.* 2015; 87:4104. [PubMed: 25818563]
36. Li S, Park Y, Duraisingham S, Strobel FH, Khan N, Soltow QA, Jones DP, Pulendran B. Predicting network activity from high throughput metabolomics. *PLoS Comput Biol.* 2013; 9:e1003123. [PubMed: 23861661]
37. Xu X, Araki K, Li S, Han JH, Ye L, Tan WG, Konieczny BT, Bruinsma MW, Martinez J, Pearce EL, Green DR, Jones DP, Virgin HW, Ahmed R. Autophagy is essential for effector CD8 T cell survival and memory formation. *Nature Immunol.* 2014; 15:1152. [PubMed: 25362489]
38. Hoffman JM, Soltow QA, Li S, Sidik A, Jones DP, Promislow DE. Effects of age, sex, and genotype on high-sensitivity metabolomic profiles in the fruit fly, *Drosophila melanogaster*. *Aging Cell.* 2014; 13:596. [PubMed: 24636523]
39. Sleator RD. The human superorganism - of microbes and men. *Med Hypotheses.* 2010; 74:214. [PubMed: 19836146]
40. Barnes S, Kirk M, Coward L. Isoflavones and their conjugates in soy foods: extraction conditions and analysis by HPLC-mass spectrometry. *J Agric Food Chem.* 1994; 42:2466.
41. Barnes S. The biochemistry, chemistry and physiology of the isoflavones in soybeans and their food products. *Lymph Res Biol.* 2010; 8:89.
42. Sfakianos J, Coward L, Kirk M, Barnes S. Intestinal uptake and biliary excretion of the isoflavone genistein in the rat. *J Nutr.* 1997; 127:1260. [PubMed: 9202077]

43. Day AJ, Cañada FJ, Díaz JC, Kroon PA, Mclauchlan R, Faulds CB, Plumb GW, Morgan MR, Williamson G. Dietary flavonoid and isoflavone glycosides are hydrolysed by the lactase site of lactase phlorizin hydrolase. *FEBS Lett.* 2000; 468:166. [PubMed: 10692580]
44. Setchell KD, Clerici C, Lephart ED, Cole SJ, Heenan C, Castellani D, Wolfe BE, Nechemias-Zimmer L, Brown NM, Lund TD, Handa RJ, Heubi JE. S-equol, a potent ligand for estrogen receptor beta, is the exclusive enantiomeric form of the soy isoflavone metabolite produced by human intestinal bacterial flora. *Am J Clin Nutr.* 2005; 81:1072. [PubMed: 15883431]
45. Le A, Lane AN, Hamaker M, Bose S, Gouw A, Barbi J, Tsukamoto T, Rojas CJ, Slusher BS, Zhang H, Zimmerman LJ, Liebler DC, Slebos RJ, Lorkiewicz PK, Higashi RM, Fan TW, Dang CV. Glucose-independent glutamine metabolism via TCA cycling for proliferation and survival in B cells. *Cell Metab.* 2012; 15:110. [PubMed: 22225880]
46. Lane AN, Fan TW, Higashi RM. Isotopomer-based metabolomic analysis by NMR and mass spectrometry. *Methods Cell Biol.* 2008; 84:541. [PubMed: 17964943]
47. Fan TW, Lane AN, Higashi RM, Farag MA, Gao H, Bousamra M, Miller DM. Altered regulation of metabolic pathways in human lung cancer discerned by (<sup>13</sup>C) stable isotope-resolved metabolomics (SIRM). *Mol Cancer.* 2009; 8:41. [PubMed: 19558692]
48. Liu W, Le A, Hancock C, Lane AN, Dang CV, Fan TW, Phang JM. Reprogramming of proline and glutamine metabolism contributes to the proliferative and metabolic responses regulated by oncogenic transcription factor c-MYC. *Proc Natl Acad Sci USA.* 2012; 109:8983. [PubMed: 22615405]
49. Yang Y, Lane AN, Ricketts CJ, Sourbier C, Wei MH, Shuch B, Pike L, Wu M, Rouault TA, Boros LG, Fan TW, Linehan WM. Metabolic reprogramming for producing energy and reducing power in fumarate hydratase null cells from hereditary leiomyomatosis renal cell carcinoma. *PLoS One.* 2013; 8:e72179. [PubMed: 23967283]
50. Sellers K, Fox MP, Bousamra M II, Slone SP, Higashi RM, Miller DM, Wang Y, Yan J, Yuneva MO, Deshpande R, Lane AN, Fan TW. Pyruvate carboxylase is critical for non-small-cell lung cancer proliferation. *J Clin Invest.* 2015; 125:687. [PubMed: 25607840]
51. McDonnell LA, Heeren RMA, de Lange RPJ, Fletcher IW. Higher sensitivity secondary ion mass spectrometry of biological molecules for high resolution, chemically specific imaging. *J Am Soc Mass Spectrom.* 2006; 17:1195. [PubMed: 16769220]
52. Guenther S, Schäfer KC, Balog J, Dénes J, Majoros T, Albrecht K, Tóth M, Spengler B, Takáts Z. Electrospray post-ionization mass spectrometry of electrosurgical aerosols. *J Am Soc Mass Spectrom.* 2011; 22:2082. [PubMed: 21952773]
53. Balog J, Sasi-Szabó L, Kinross J, Lewis MR, Muirhead LJ, Veselkov K, Mirnezami R, Dezső B, Damjanovich L, Darzi A, Nicholson JK, Takáts Z. Intraoperative tissue identification using rapid evaporative ionization mass spectrometry. *Sci Transl Med.* 2013; 5:194ra93.
54. Golf O, Strittmatter N, Karancsi T, Pringle SD, Speller AV, Mroz A, Kinross JM, Abbassi-Ghadi N, Jones EA, Takats Z. Rapid evaporative ionization mass spectrometry imaging platform for direct mapping from bulk tissue and bacterial growth media. *Anal Chem.* 2015; 87:2527. [PubMed: 25671656]
55. Wiseman JM, Ifa DR, Zhu Y, Kissinger CB, Manicke NE, Kissinger PT, Cooks RG. Desorption electrospray ionization mass spectrometry: Imaging drugs and metabolites in tissues. *Proc Natl Acad Sci USA.* 2008; 105:18120. [PubMed: 18697929]
56. Guenther S, Muirhead LJ, Speller AV, Golf O, Strittmatter N, Ramakrishnan R, Goldin RD, Jones E, Veselkov K, Nicholson J, Darzi A, Takats Z. Spatially resolved metabolic phenotyping of breast cancer by desorption electrospray ionization mass spectrometry. *Cancer Res.* 2015; 75:1828. [PubMed: 25691458]
57. Gerbig S, Golf O, Balog J, Denes J, Baranyai Z, Zarand A, Raso E, Timar J, Takats Z. Analysis of colorectal adenocarcinoma tissue by desorption electrospray ionization mass spectrometric imaging. *Anal Bioanal Chem.* 2012; 403:2315. [PubMed: 22447214]
58. Khatib-Shahidi S, Andersson M, Herman JL, Gillespie TA, Caprioli RM. Direct molecular analysis of whole-body animal tissue sections by imaging MALDI mass spectrometry. *Anal Chem.* 2006; 78:6448. [PubMed: 16970320]

59. Stoyanovsky DA, Sparvero LJ, Amoscato AA, He RR, Watkins S, Pitt BR, Bayir H, Kagan VE. Improved spatial resolution of matrix-assisted laser desorption/ionization imaging of lipids in the brain by alkylated derivatives of 2,5-dihydroxybenzoic acid. *Rapid Commun Mass Spectrom*. 2014; 28:403. [PubMed: 24497278]
60. Rao S, Walters KB, Wilson L, Chen B, Bolisetty S, Graves D, Barnes S, Agarwal A, Kabarowski JH. Early lipid changes in acute kidney injury using SWATH lipidomics coupled with MALDI tissue imaging. *Am J Physiol Renal Physiol*. 2016 Feb 24. *ajprenal.00100.2016*. doi: 10.1152/ajprenal.00100.2016. [Epub ahead of print].
61. Anderson DM, Ablonczy Z, Koutalos Y, Spraggins J, Crouch RK, Caprioli RM, Schey KL. High resolution MALDI imaging mass spectrometry of retinal tissue lipids. *J Am Soc Mass Spectrom*. 2014; 25:1394. [PubMed: 24819461]
62. Buck A, Ly A, Balluff B, Sun N, Gorzolka K, Feuchtinger A, Janssen KP, Kuppen PJ, van de Velde CJ, Weirich G, Erlmeier F, Langer R, Aubele M, Zitzelsberger H, Aichler M, Walch A. High-resolution MALDI-FT-ICR MS imaging for the analysis of metabolites from formalin-fixed, paraffin-embedded clinical tissue samples. *J Pathol*. 2015; 237:123. [PubMed: 25965788]
63. Thompson DK, Sloane R, Bain JR, Stevens RD, Newgard CB, Pieper CF, Kraus VB. Daily variation of serum acylcarnitines and amino acids. *Metabolomics*. 2012; 8:556. [PubMed: 25067934]
64. Layman CA, Araujo MS, Boucek R, Hammerschlag-Peyer CM, Harrison E, Jud ZR, Matich P, Rosenblatt AE, Vaudo J, Yeager LA, Post DM, Bearhop S. Applying stable isotopes to examine food web structure: an overview of analytical tools. *Biological Reviews*. 2012; 87:545. [PubMed: 22051097]
65. Nikolskiy I, Siuzdak G, Patti GJ. Discriminating precursors of common fragments for large-scale metabolite profiling by triple quadrupole mass spectrometry. *Bioinformatics*. 2015; 31:2017. [PubMed: 25691443]
66. Desmet G, Callewaert M, Ottevaere H, De Malsche W. Merging open-tubular and packed bed liquid chromatography. *Anal Chem*. 2015; 87:7382. [PubMed: 26075679]



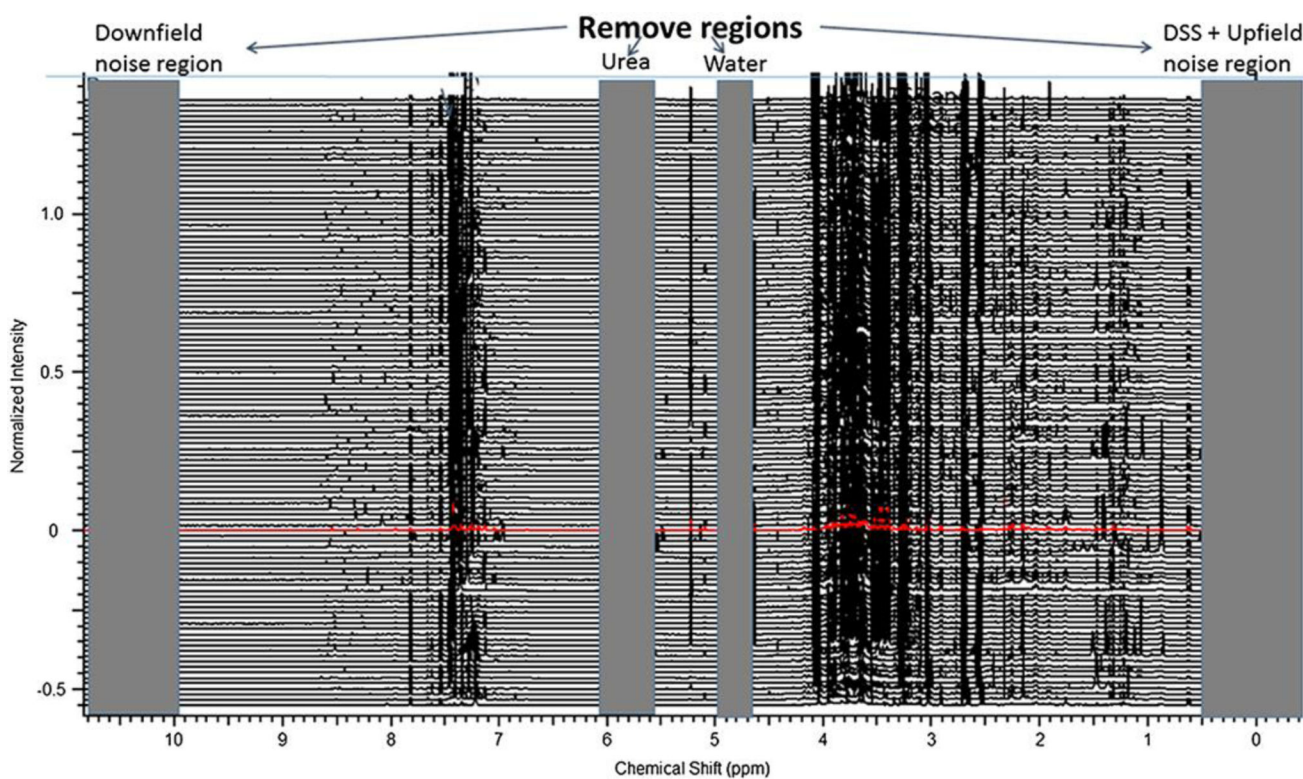


**Figure 1. Aligned, multiple NMR spectra with regions marked that can be deleted prior to NMR binning**

The spectra are divided into regular small regions (0.04 ppm) called bins. As noted on this figure, NMR resonances with downfield chemical shifts (> 9 ppm, noise), urea resonances (5.4–6 ppm), the suppressed water resonance (4.8–5 ppm) and resonances in the upfield region (<0.4 ppm, noise and DSS) are removed from the dataset prior to binning. Binned NMR data are usually normalized to the total integral of each of the spectrum.



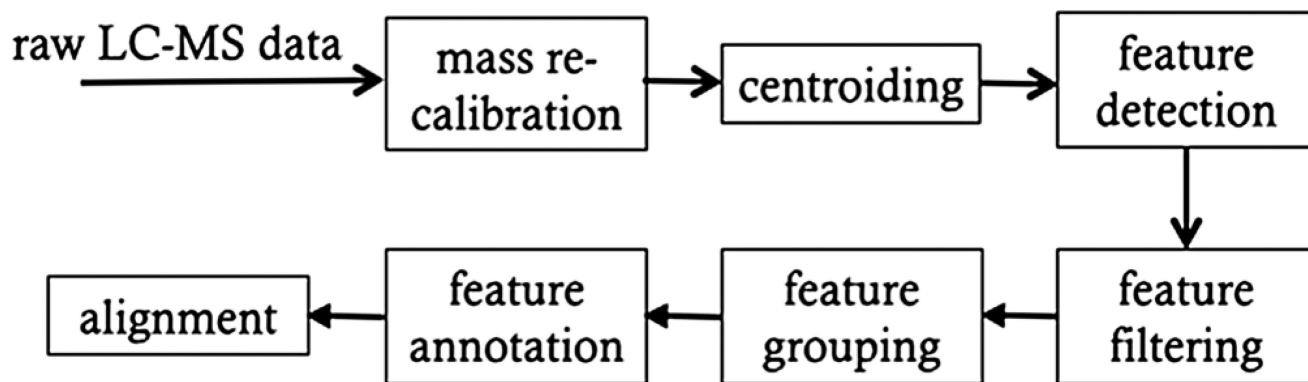


**Figure 2. Workflow for pre-processing LC-MS and GC-MS data**

The collected data are first centroided to obtain the best estimates of the masses of the ions. This is followed by detection of features (i.e., peaks) and their grouping and alignment between different samples. This allows the areas of the aligned peaks to be compared statistically.

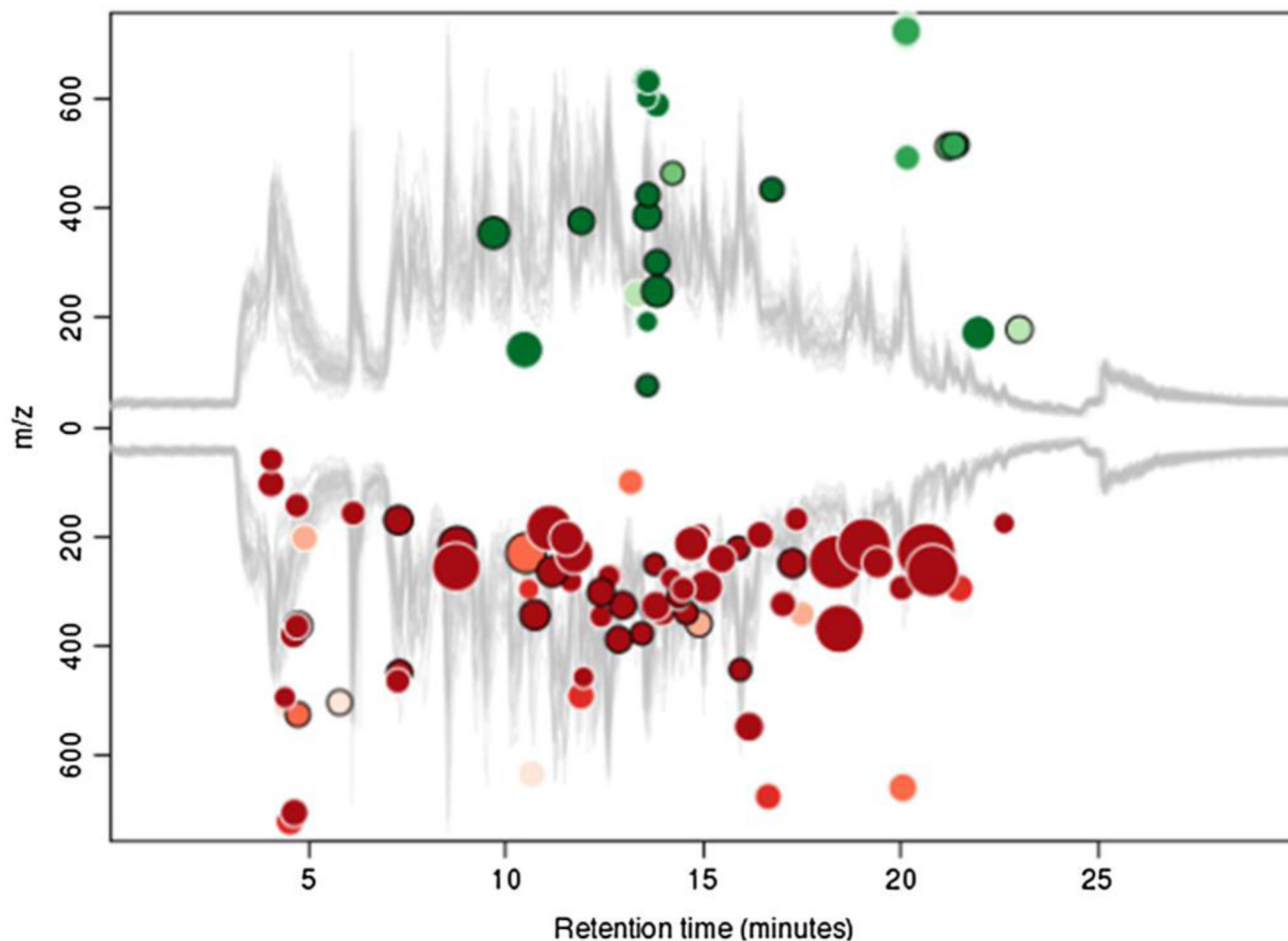


**Figure 3. A Cloud plot used to visualize LC-MS data**

This plot is generated by XCMSOnline (<https://xcmsonline.scripps.edu>). The two gray traces are the overlaid total ion chromatograms from all the samples being analyzed. Ions considered to be statistically different using fold change  $>1.5$  (up or down) and  $p < 0.01$  are marked as circles coded for up-regulated (green) or down-regulated (red). The size of the circles represents the absolute value of the  $\log_2(\text{fold change})$  and the depth of the color the  $-\log(p\text{-value})$ . The online analysis also includes an interactive form of the plot where clicking on each dot with a mouse reveals a box containing the  $m/z$  value, retention time,  $p$ -value, fold change, maximum intensity and where known, the identity of the ion.



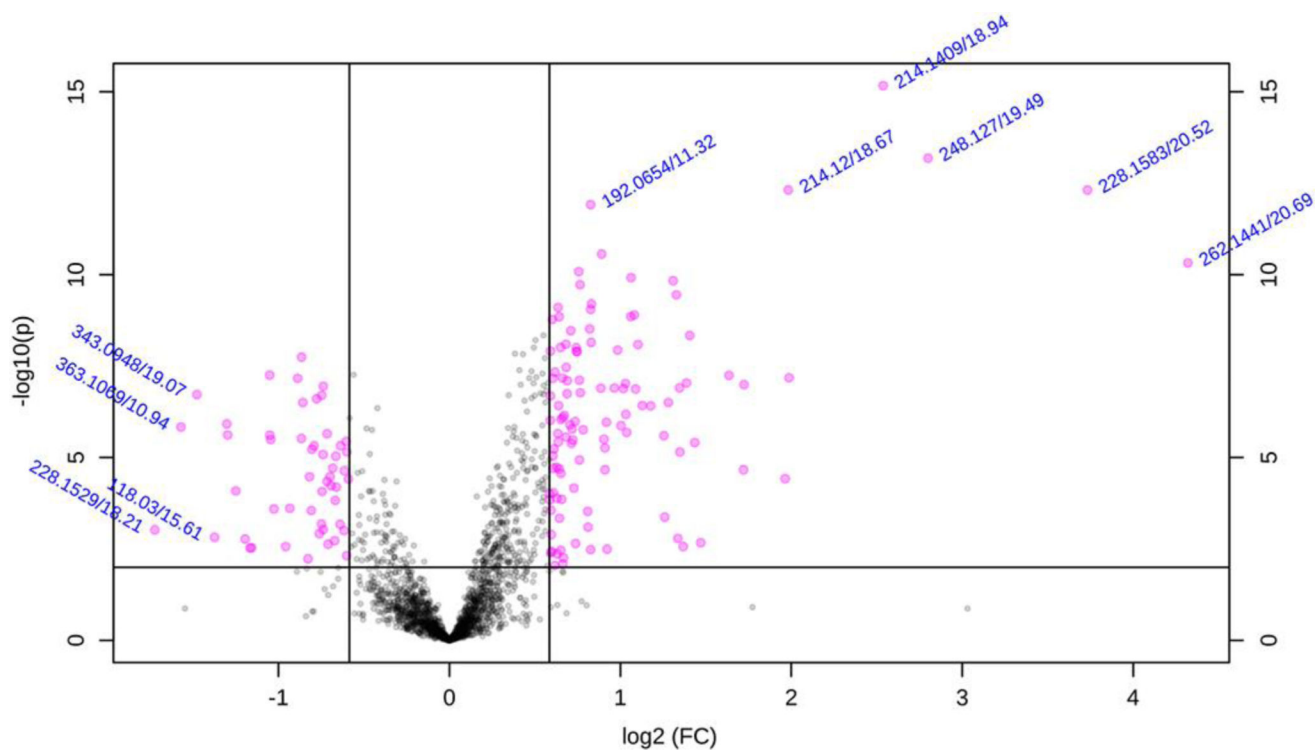


**Figure 5. Univariate Analysis Volcano plot**

The negative logarithm of the p-value for each metabolite is plotted against the logarithm to the base 2 of the fold change.

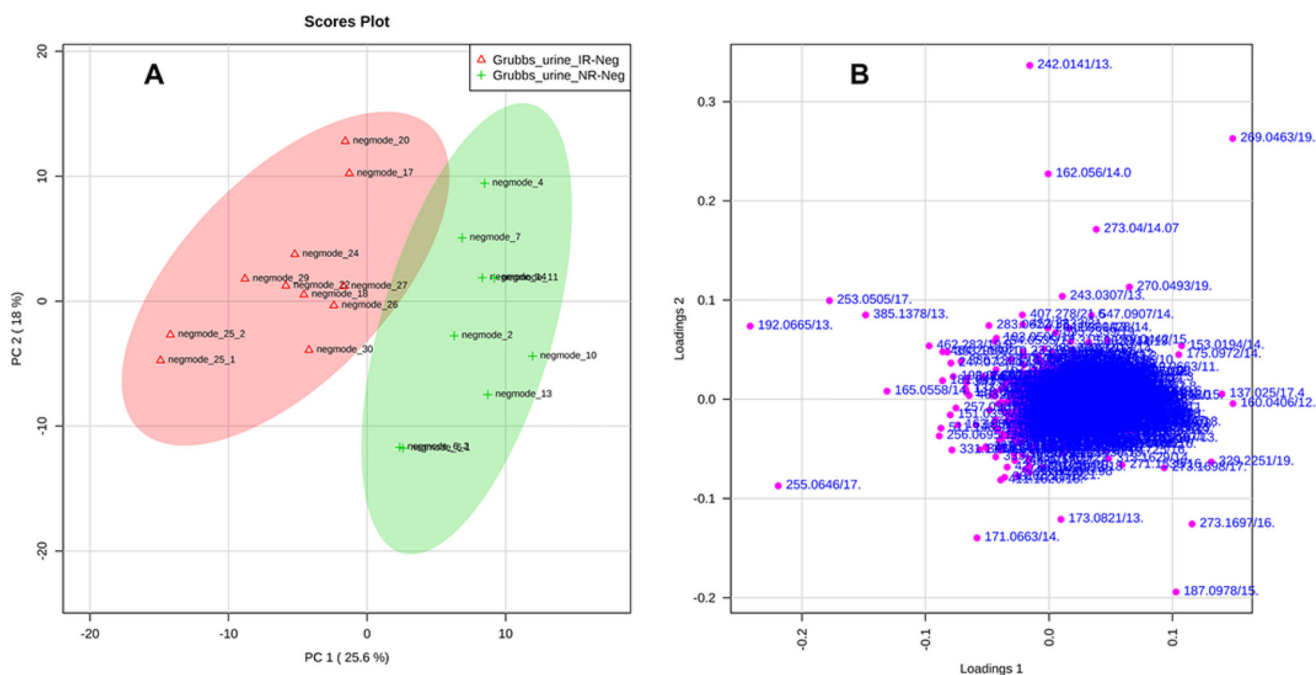


**Figure 6. Principal components analysis (PCA)**

PCA analysis allows for the separation of the variation between samples to be separate into several principal components. It does not use group information to do this. The contribution of each metabolite in a sample to a principal component allows reduction of 1,000 or more factors into a single number representing that component. (A) By plotting these numbers for a sample in 2D-PCA or 3D-PCA formats and then color coding the point with the group they are derived from, allows the investigator to determine if there is a group separation. In the example in this figure the 95% confidence for each group is also marked. (B) The loadings plot provides information on which ions are contributing the most to the separations between the groups.

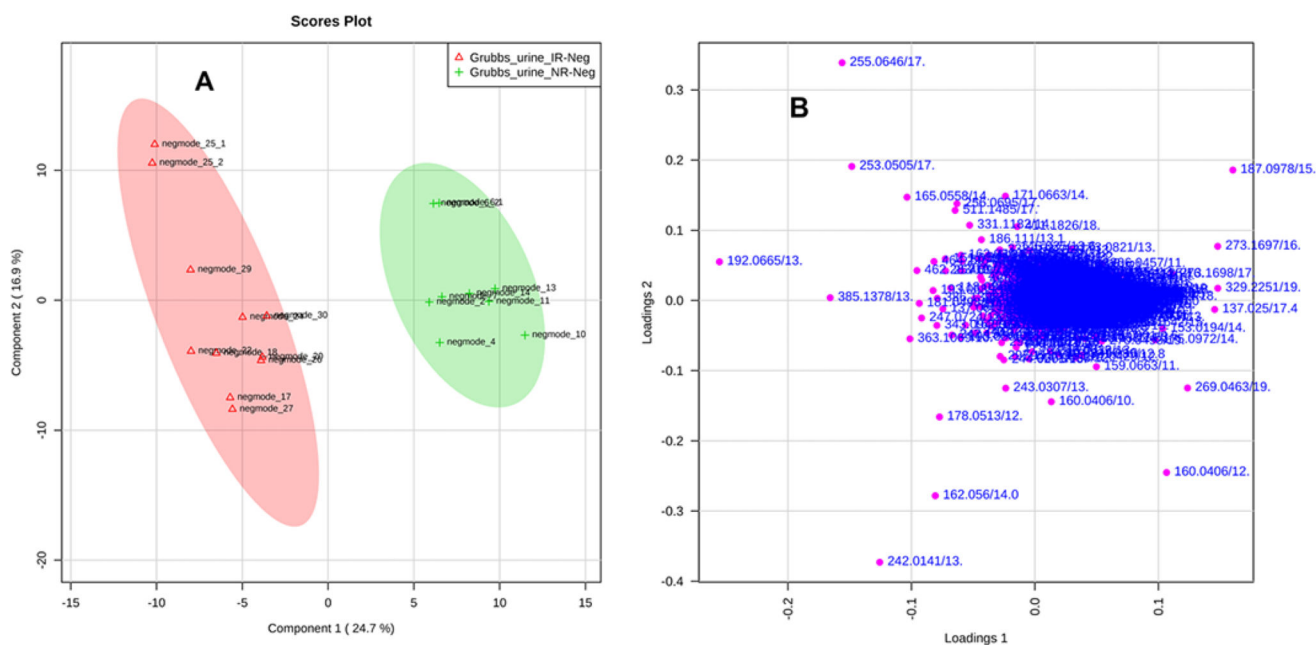


**Figure 7. Partial Least Squares-Discriminant Analysis (PLS-DA)**

This form of analysis, unlike PCA analysis, is a supervised method. It, too, breaks down the total variation into factors that are single numbers representing the contribution of each metabolite to the factor. These, as before for PCA analysis, can be examined as 2D- or 3D-plots (A) and loading plots (B).



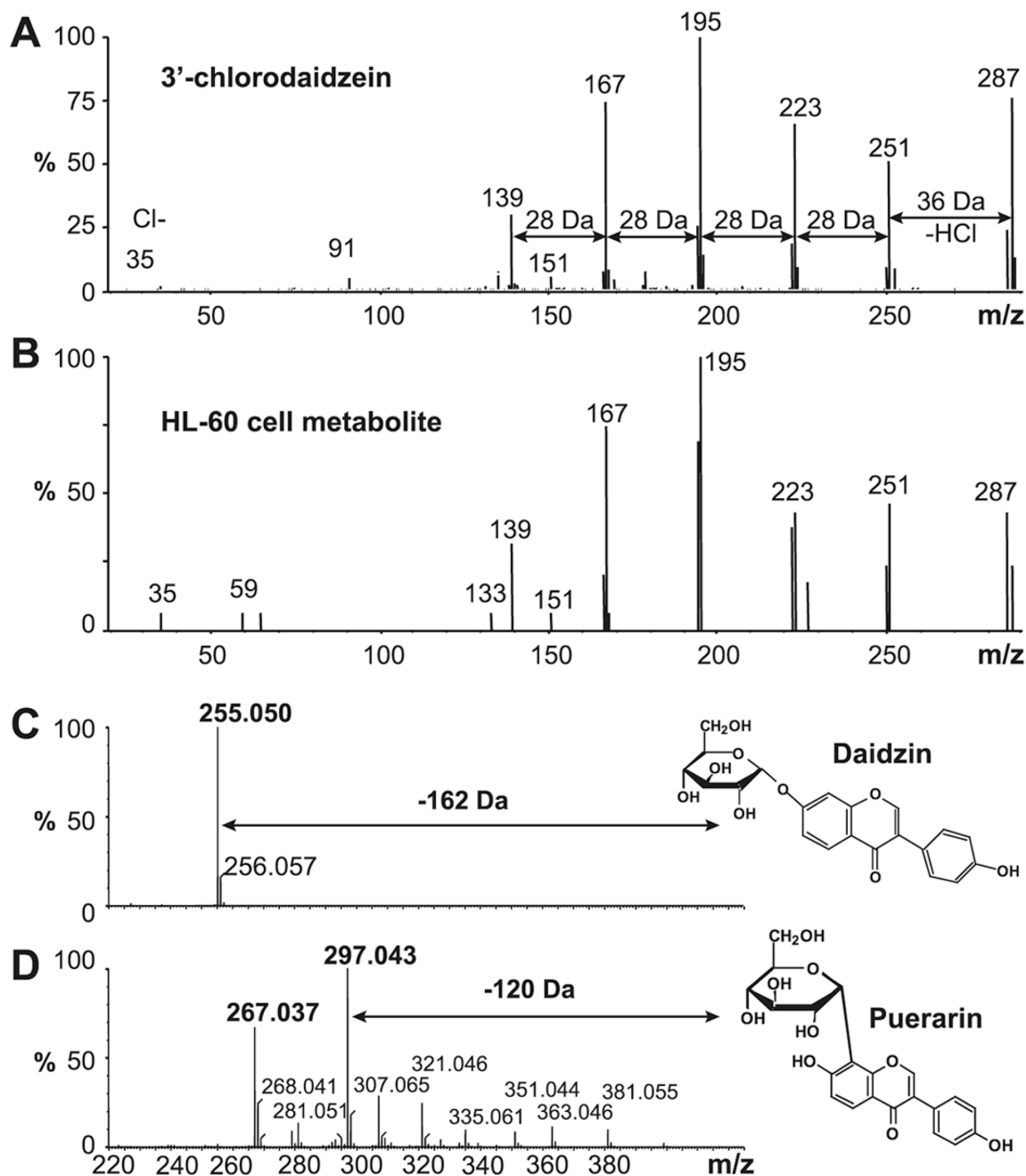


**Figure 8. Interpreting MS/MS spectra**

In the upper example, the MS/MS spectrum of authentic 3'-chlorodaidzein [A] is shown above the MS/MS spectrum of the HL-60 cell metabolite [B]. Characteristic product ions are due to losses of HCl (–36 Da) and C=O (–28 Da). In the lower example, there are marked differences in the MS/MS spectra of daidzein conjugated to glucose in two different ways. When the link is through a C-O-C bond (daidzin), the intact glucose moiety is cleaved off – a neutral loss of 162 Da leaving the aglycone ion ( $m/z$  255) [C]. However, when the bond linking daidzein and glucose is a carbon-carbon bond (in the daidzein-8C-glucoside,

puerarin), the glucose moiety is retained and the observed ions are due to water losses and other rearrangements of the glucose moiety [D].

Author Manuscript

Author Manuscript

Author Manuscript

Author Manuscript

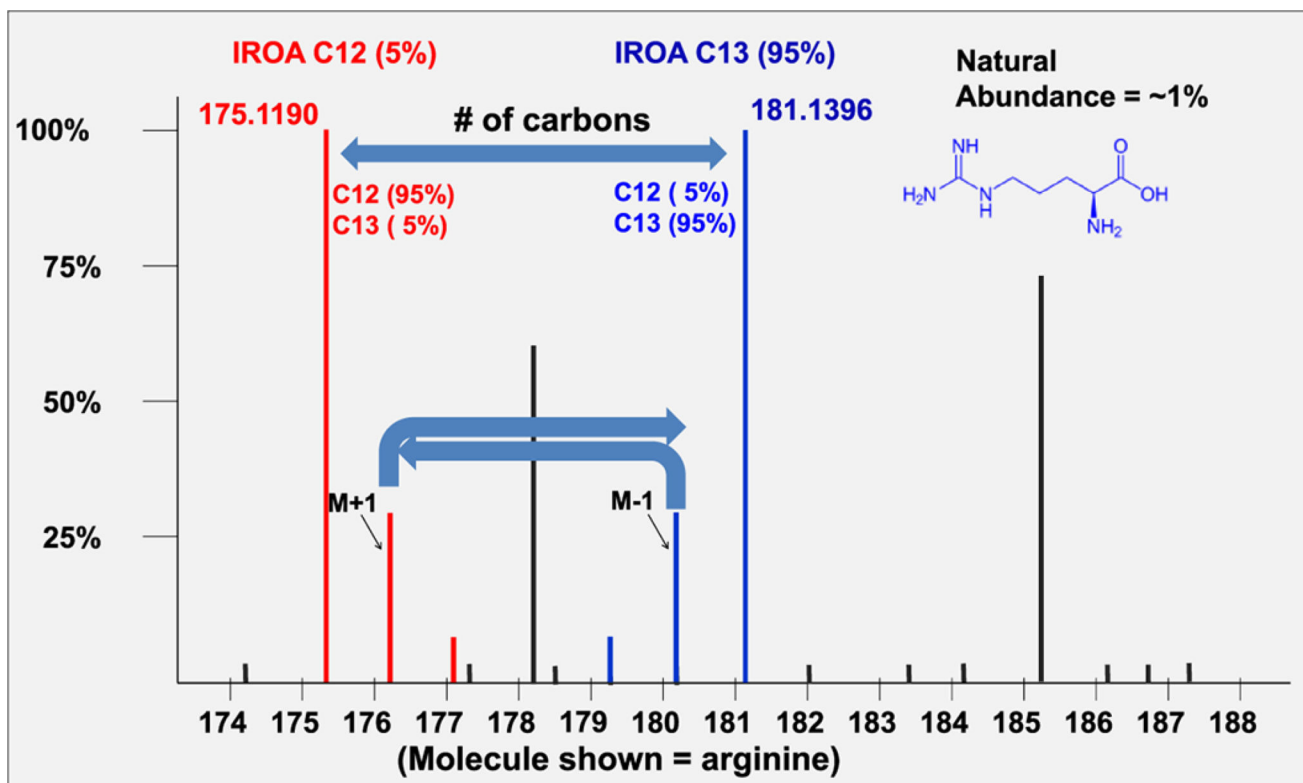


**Figure 9. Isotope ratio Outlier Analysis (IROA)**

The IROA approach uses two sets of distinct randomized substrates, labeled with 95%  $^{13}\text{C}$  and 5%  $^{13}\text{C}$ , to individually label cellular metabolomes with and without stressors. Pooled cells are processed and MS analysis reveals U-shaped mirrored isotopologue pairs of metabolites. The width of the U in Da (distance between the monoisotopic  $^{12}\text{C}$  and  $^{13}\text{C}$  ion pairs) gives the number of carbon atoms in the metabolite. (Permission provided by IROA Technologies).

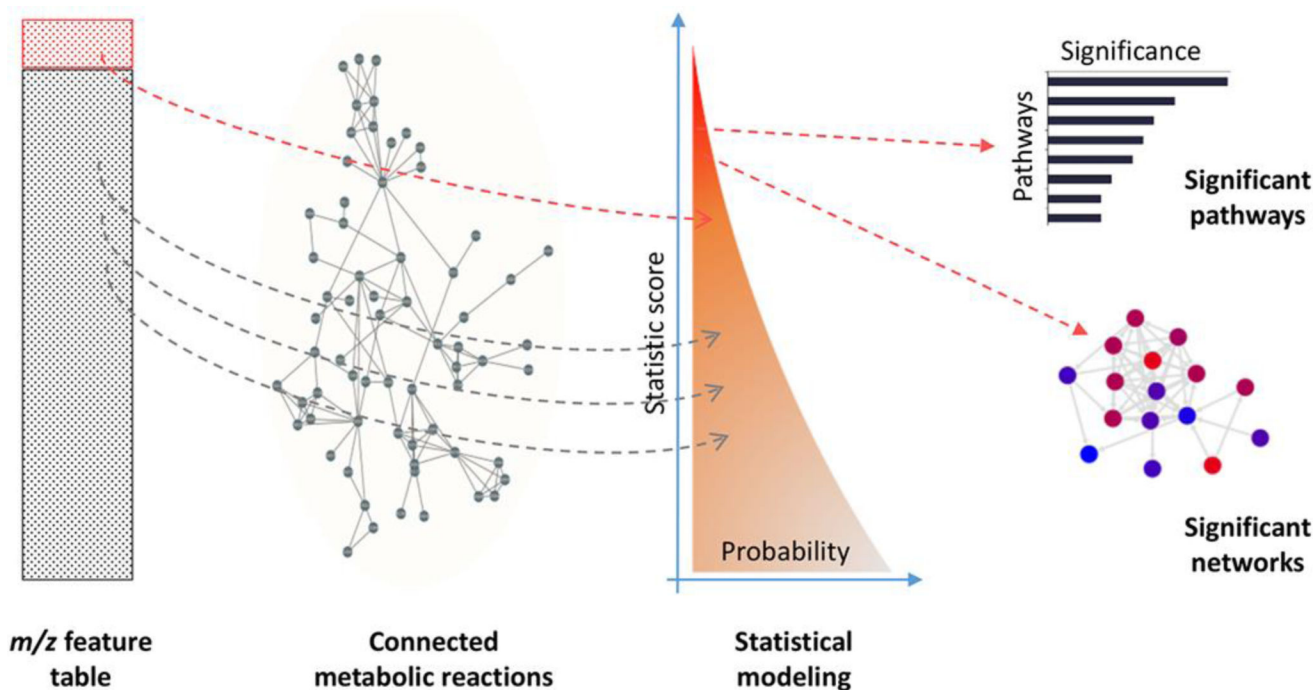


**Figure 10. Mummichog analysis of LC-MS and GC-MS data to discover metabolite networks and pathway associations**

This analysis is a selectable item (Connections) on the XCMSonline website, or it can be run in the command line mode after first downloading the Mummichog software. The latter is helpful when metabolomics data require normalization, mean centering and scaling prior to statistical analysis. The user creates a .txt file of all the metabolites, their  $m/z$  values, their  $t$ -test values and their  $p$ -values (A). This file is used to determine networks of connected reactions (B). After statistical modeling (C) to estimate random association with metabolomic pathways, pathways and networks that are enriched by the significantly different ions are identified (D).

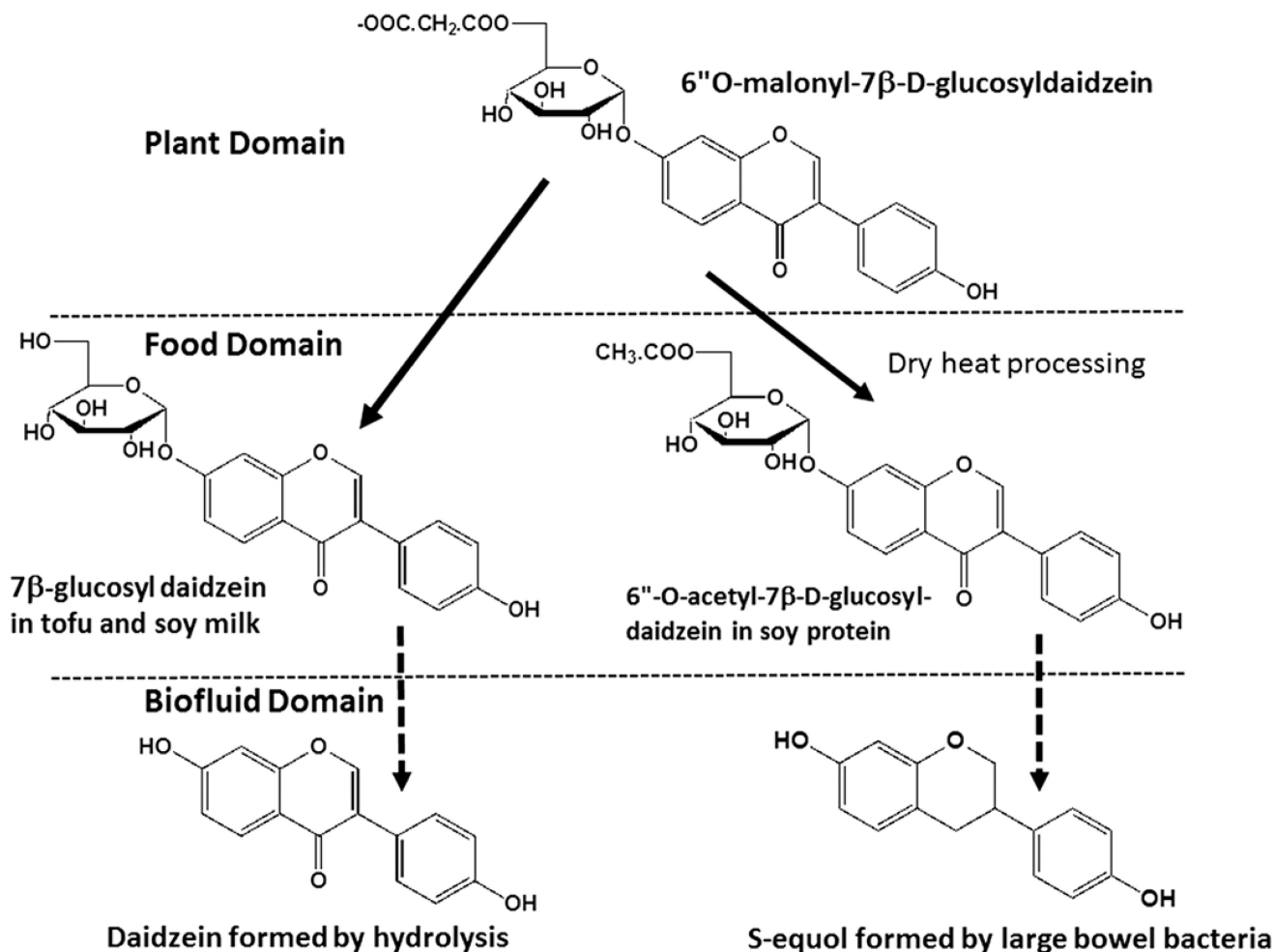


**Figure 11. Complex pathways of metabolism of the isoflavone daidzein across several biological domains**

Isoflavones are synthesized in the soybean and converted to their  $\beta$ -glucosides which in turn are esterified with malonic acid and stored in vacuoles in the soybean seed. Harvested soybeans are soaked in water (to remove protease inhibitors) and ground and treated with hot boiling water to extract the proteins therein thereby forming soy milk. Soy milk is coagulated (not shown) to form tofu. This treatment causes hydrolysis of the malonate ester group and yields the  $\beta$ -glucoside, 7 $\beta$ -D-glucosyl daidzein. When this form of daidzein is consumed (in tofu or soymilk), it is enzymatically hydrolyzed by a physiologic enzyme in the small intestine to unconjugated daidzein. The latter is absorbed into the enterocyte where it mostly undergoes  $\beta$ -glucuronidation before entering the blood stream. In contrast, soybeans in many countries such as the USA are a rich source of polyunsaturated oil. Once the soybeans have been defatted they can be converted into protein products. In order to inactivate residual enzymes in the defatted soybean, they are subjected to toasting, a dry heating process. This causes decarboxylation of the malonate ester forming an acetate ester of 7 $\beta$ -D-glucosyl daidzein. This isoflavone conjugate when eaten is not a substrate for the physiologic enzyme and instead makes its way to the large bowel where hydrolysis is caused by colonic bacteria.

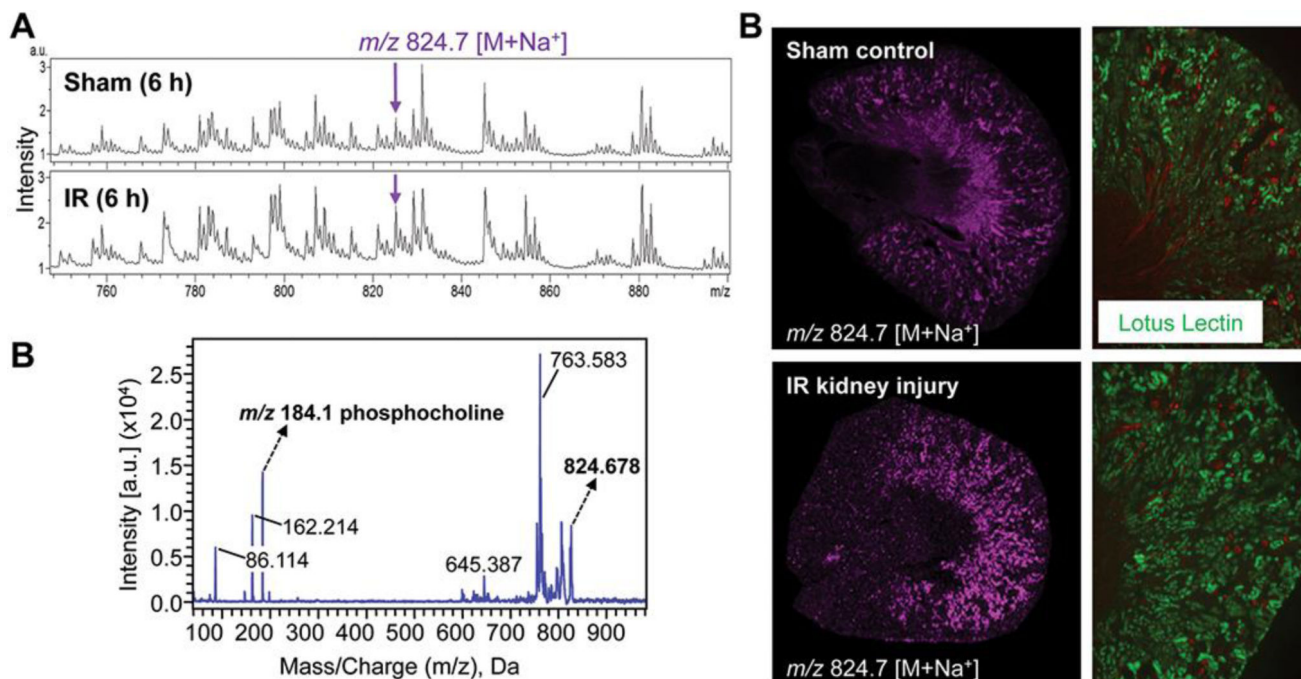


### Figure 12. Imaging mass spectrometry of early kidney injury

Early (6 h) increases in renal levels of an ether-linked phosphatidylcholine (PC O-38:1) with ischemia reperfusion (IR) kidney injury (identified using SWATH lipidomics) are predominantly localized to proximal tubules. (A) MALDI-IMS spectra from control and IR kidneys. Arrow denotes ion at  $m/z$  824.7 consistent with sodiated ( $[M+Na^+]$ ) PC O-38:1. (B) Positive ion mode MALDI-IMS images of 2,5-DHB coated coronal kidney cryosections from control and IR mice showing the distribution of  $m/z$  824.7 sodiated PC O-38:1. Lotus tetragonolobus lectin staining of proximal tubules in coronal kidney sections adjacent to those in (A) shown alongside demonstrate that PC O-38:1 is most abundant in proximal tubular areas. (C) Positive mode MS/MS analysis on 2,5-DHB coated kidney cryosections of  $m/z$  824.7  $[M+Na^+]$  ion showing a  $m/z$  184.1 fragment indicative of the PC headgroup in PC O-38:1.